Acta Crystallographica Section F
Structural Biology and Crystallization Communications
ISSN 1744-3091

Characterization of crystals of an antibody-recognition fragment of the cancer differentiation antigen mesothelin in complex with the therapeutic antibody MORAb-009

Jichun Ma,[a]‡ Wai Kwan Tang,[a] Lothar Esser,[a] Ira Pastan[b] and Di Xia[a]*

[a]Laboratory of Cell Biology, Center for Cancer Research, National Institutes of Health, Bethesda, MD 20892, USA, and [b]Laboratory of Molecular Biology, Center for Cancer Research, National Institutes of Health, Bethesda, MD 20892, USA

‡ Current address: Janssen Research and Development LLC, Spring House, PA 19477, USA.

Correspondence e-mail: dixia@helix.nih.gov

Received 9 May 2012
Accepted 21 June 2012

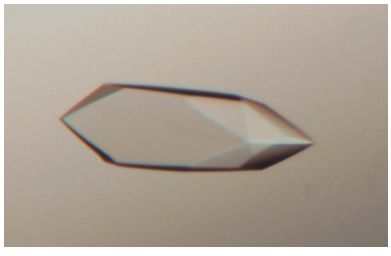

The mesothelin-specific monoclonal antibody MORAb-009 is capable of blocking the binding of mesothelin to CA-125 and displays promising anticancer potential. It is currently undergoing clinical trials. In order to understand the basis of the interaction between MORAb-009 and mesothelin at atomic resolution, both the Fab fragment of MORAb-009 and the complex between the Fab and an N-terminal fragment of mesothelin (residues 7–64) were crystallized. The crystals of the Fab diffracted X-rays to 1.75 Å resolution and had the symmetry of space group $P4_12_12$, with unit-cell parameters $a = b = 140.6$, $c = 282.0$ Å. The crystals of the mesothelin–Fab complex diffracted to 2.6 Å resolution and belonged to the hexagonal space group $P6_4$, with unit-cell parameters $a = b = 146.2$, $c = 80.9$ Å. Structural analyses of these molecules are in progress.

1. Introduction

Mesothelin is a 40 kDa C-terminally glycosylphosphatidylinositol-anchored glycoprotein that is present on the surface of a number of cells, including normal mesothelial cells and many cancer cells, including mesothelioma, ovarian, pancreatic, lung, stomach and liver cancer cells (Chang & Pastan, 1996). It is synthesized as a 69 kDa precursor protein which is subsequently processed to yield membrane-bound mesothelin (Chang & Pastan, 1996) and another 31 kDa mature product known as megakaryocyte-potentiating factor (Kojima *et al.*, 1995). Mesothelin is now considered to be a tumor differentiation antigen because it is expressed at low levels in a restricted set of normal adult tissues such as the mesothelium, but is aberrantly overexpressed in a variety of tumors including mesothelioma, ovarian cancer, pancreatic cancer and lung cancer (Hassan *et al.*, 2004; Ho *et al.*, 2007). Although the cellular function of mesothelin remains unclear, recent studies have shown that it binds to CA-125 (MUC16) and that this interaction may mediate cell adhesion, suggesting a role in cancer metastasis (Rump *et al.*, 2004). Indeed, CA-125 is a well documented biomarker for ovarian cancer (Bast *et al.*, 1998) and its expression on the cell membrane has also been reported in the majority (88%) of mesothelioma cases (Bateman *et al.*, 1997). These data suggest that mesothelin may partner with CA-125 to perform its functions.

Since mesothelin is specifically expressed in malignant tumors, it is likely to be a target for anticancer agents. It has been noted that the level of mesothelin-specific antibodies was elevated in the sera of patients with mesothelioma and epithelial ovarian cancer and that this elevation was associated with high expression of mesothelin in tumors (Ho *et al.*, 2005). Antibody response to mesothelin-expressing ovarian carcinoma cells may be one of the mechanisms for reducing tumor load, contributing to prolonged survival (Yen *et al.*, 2006). The development of therapeutic antibodies against mesothelin is therefore of major importance (Chowdhury & Pastan, 1999). A promising antibody with potential clinical application is MORAb-009, a chimeric IgG1/κ antibody that was generated by fusing the genes encoding the anti-mesothelin Fv (SS1 scFv) in frame with human IgG1 and κ constant regions (Hassan *et al.*, 2007). Animal experiments have shown that MORAb-009 in combination with chemotherapy leads to a marked reduction in tumor growth of mesothelin-expressing tumors (Hassan *et al.*, 2007). Clinical studies

demonstrated that the use of MORAb-009 increased the serum level of CA-125, most likely owing to blocking its binding to mesothelin, which can be used as a strategy to prevent tumor metastasis (Hassan *et al.*, 2010). Currently, this antibody is undergoing a phase II clinical trial. Other applications of mesothelin-specific antibodies have also been documented, including targeted delivery of cytotoxic agents that are covalently attached to the antibodies (Pastan *et al.*, 2006).

One of the critical factors that affect the efficacy of an antibody in clinical application is its binding affinity towards its antigen. Gaining access to atomic resolution information about the interaction between mesothelin and the antibody is highly desirable for further improvement of the anti-mesothelin antibody. However, structural information for mesothelin has been limited to a molecular-modeling study (Sathyanarayana *et al.*, 2009), which predicted a superhelical structure, and an experimental structure has yet to be obtained. Here, we report the expression, crystallization and X-ray diffraction experiments on crystals of both the Fab fragment of MORAb-009 and the complex of Fab with an N-terminal fragment that includes residues 7–64 of mesothelin (Msln7-64).

2. Materials and methods

2.1. Preparation of the Fab fragment from IgG

MORAb-009 IgG was obtained from Morphotek Inc. (Exton, Pennsylvania, USA). The Fab fragment was prepared using the Fab preparation kit from Thermo Scientific (Rockford, Illinois, USA). Briefly, 0.5 ml MORAb-009 IgG at 5 mg ml^{-1} was first passed through a desalting column pre-equilibrated with the supplied digestion buffer (the pH was adjusted to 7 with cysteine–HCl). The IgG was then digested by mixing it with 0.125 ml resin-immobilized papain and incubating at 310 K for 4 h. The treated material was recovered and subsequently incubated on a Protein A column to remove the Fc fragments and undigested IgG. Finally, the Fab fragments were eluted with PBS buffer (100 m*M* sodium phosphate, 150 m*M* sodium chloride pH 7.2). The purified Fab fragments in PBS buffer from 4 ml IgG were pooled and concentrated to 8 mg ml^{-1} using an Amicon Ultra concentrator (Millipore, Billerica, Masssachusetts, USA) with a molecular-weight cutoff of 30 kDa. The resulting sample can be directly used for crystallization or for the preparation of the Fab–mesothelin N-terminal fragment complex.

2.2. Production of the Msln7-64 fragment

We had previously constructed a plasmid for expressing the fusion protein of thioredoxin (TrxA) with mesothelin N-terminal residues 1–64 in the vector pET32a. Based on this plasmid, we removed the DNA coding region for TrxA and the first six amino-acid residues of mesothelin; we also added a GSLEHHHHHH tag at the C-terminus, thus completing a new plasmid for expressing the sequence corresponding to residues 7–64 (Msln7-64). This plasmid was transformed into *Escherichia coli* strain Origami B. The cell culture was grown to an OD_{600} of 0.8 before the expression of recombinant protein was induced at 310 K for 4 h by adding isopropyl β-D-1-thiogalactopyranoside (IPTG) to 1 m*M*. The cells were harvested by centrifugation and the pellets were suspended in lysis buffer consisting of 100 m*M* Tris–HCl pH 7.5, 150 m*M* NaCl, 1 m*M* PMSF and lysed by passing them twice through a French press at a pressure of 103 MPa. The cell lysate was centrifuged at 15 000*g* for 30 min to remove unbroken cells, and the resulting supernatant was mixed with Ni–NTA resin (Qiagen, Valencia, California, USA) pre-equilibrated with washing buffer consisting of 25 m*M* Tris–HCl pH 7.5, 150 m*M* NaCl, 10% glycerol, 20 m*M* imidazole pH 7.5 and incubated for 2 h at 277 K. The resin was then transferred into a column. After washing the column with the washing buffer, the bound protein was eluted with the same buffer containing 300 m*M* imidazole. The eluate was concentrated and further purified by size-exclusion chromatography on a Superdex S-200 column equilibrated with running buffer consisting of 25 m*M* Tris–HCl pH 7.5, 150 m*M* NaCl, 2% glycerol. Fractions containing the mesothelin fragment were pooled and stored at 277 K for later use.

2.3. Protein-complex formation and purification

To prepare the Fab–Msln7-64 complex, purified Fab in PBS was mixed with Msln7-64 in a 1:2 molar ratio in buffer consisting of 25 m*M* Tris–HCl pH 7.5, 150 m*M* NaCl, 2% glycerol and the resulting mixture was incubated at 277 K overnight. Excess Msln7-64 and impurities were removed using a Superdex S-200 column with a running buffer consisting of 25 m*M* Tris–HCl pH 7.5, 150 m*M* NaCl, 2% glycerol. Each eluted fraction was checked with SDS–PAGE

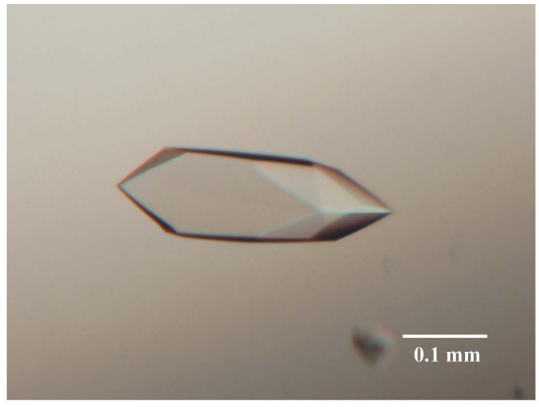

(*a*)

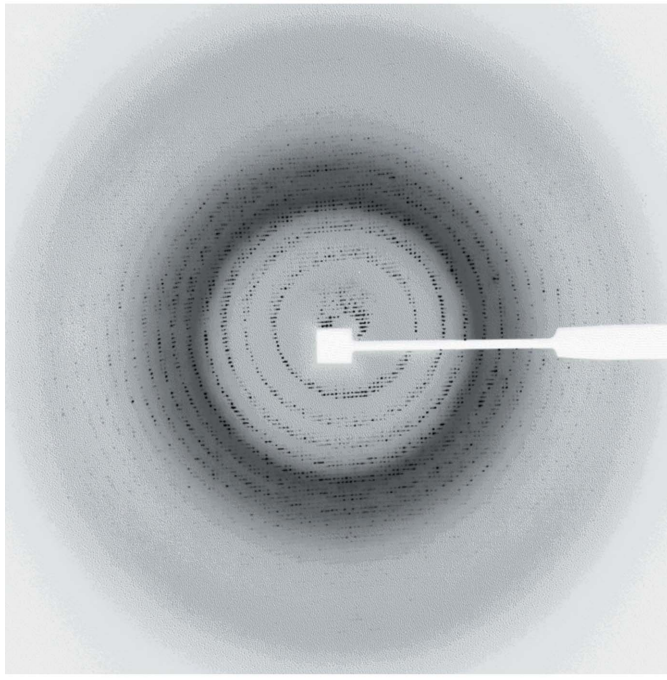

(*b*)

Figure 1
Crystal of the Fab fragment of MORAb-009 and its X-ray diffraction pattern. (*a*) A crystal of the Fab fragment derived from the hybrid monoclonal antibody MORAb-009. (*b*) An X-ray diffraction image from the crystal.

Table 1
Statistics for X-ray diffraction data sets.

Values in parentheses are for the outermost shell.

Data set	Fab (MORAb-009)	Fab–Msln7-74 complex
Wavelength (Å)	1.0	1.0
Space group	$P4_12_12$	$P6_4$
Unit-cell parameters (Å, °)	$a = b = 140.6$, $c = 282.0$	$a = b = 146.2$, $c = 80.9$
Resolution (Å)	39.1–1.75 (1.81–1.75)	50.0–2.61 (2.70–2.61)
Wilson B factor (Å^2)	18.5	45.4
No. of observations	1436883	186593
No. of unique reflections	262387	29264
Multiplicity	5.5 (2.1)	6.4 (2.4)
Completeness (%)	92.0 (70.7)	97.8 (80.0)
$R_{\rm merge}$† (%)	9.2 (40.7)	10.1 (44.2)
Mean $I/\sigma(I)$	19.5 (1.4)	22.4 (1.8)

† $R_{\rm merge}$ is defined as $\sum_{hkl}\sum_i |I_i(hkl) - \langle I(hkl)\rangle|/\sum_{hkl}\sum_i I_i(hkl)$, where $I_i(hkl)$ is the intensity of the ith observation of a reflection with Miller indices hkl and $\langle I(hkl)\rangle$ is the mean intensity for all measured $I_i(hkl)$ and Friedel pairs.

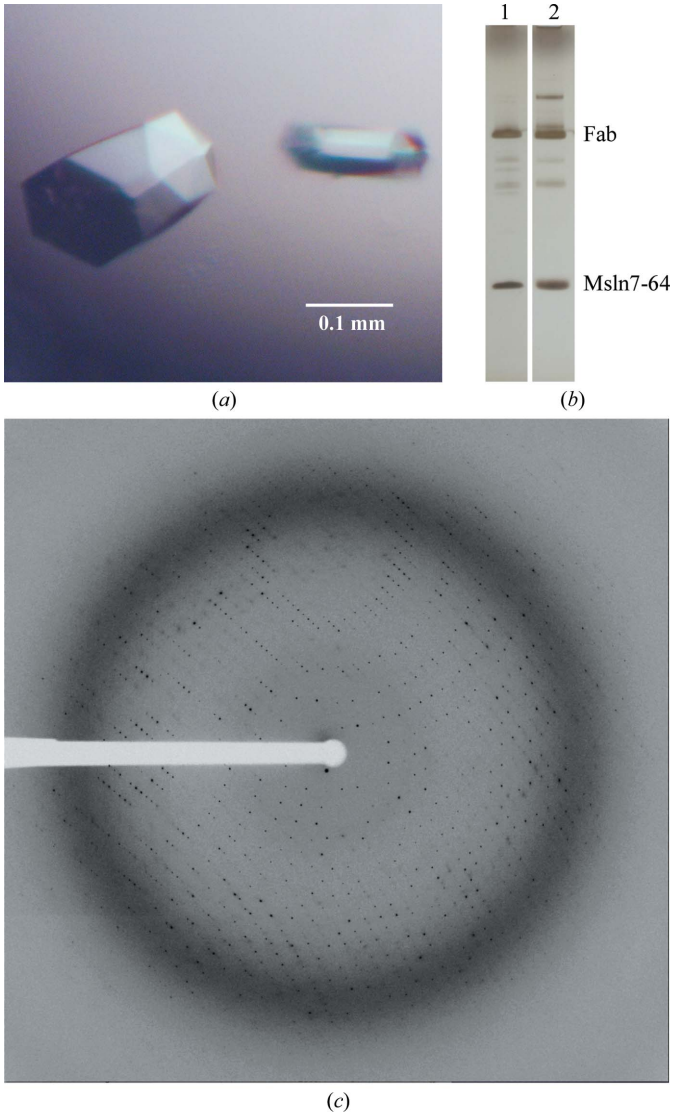

Figure 2
Crystals and diffraction image of the Fab–Msln7-64 complex. (*a*) Crystals of the complex between the Fab and Msln7-64. (*b*) SDS–PAGE analysis of the Fab–Msln7-64 complex and a crystal of the complex. Lane 1 contains the protein-complex sample before crystallization. Lane 2 is a sample from a crystal of the Fab–Msln7-64 complex after extensive washing with well solution. Samples were analyzed under nonreducing conditions and the gel was silver stained. (*c*) Diffraction image from a crystal of the complex.

and those containing the complex were pooled and concentrated to 8 mg ml^{-1} for crystallization.

2.4. Crystallization and X-ray diffraction data collection

Crystallization screening was carried out robotically by a Mosquito liquid dispenser (TTP LabTech, Cambridge, Massachusetts, USA) using the hanging-drop vapour-diffusion method in a 96-well format with commercial high-throughput screening kits (Hampton Research, Aliso Viejo, California, USA; Emerald BioSystems, Bainbridge Island, Washington, USA; Molecular Dimensions, Apopka, Florida, USA). Subsequent optimizations were performed manually by mixing 1.5 µl protein solution with 1.5 µl precipitant solution and equilibrating the mixture against 500 µl reservoir solution using the hanging-drop vapour-diffusion method at 294 K. Crystallization parameters optimized included the concentration of precipitants, the pH and the use of various types of additives. Crystallization well solutions supplemented with different concentrations of glycerol, various PEGs, sucrose and salts were tested for cryoprotection of Fab–mesothelin crystals by dipping the crystals directly into the solutions for various lengths of time followed by cooling in liquid nitrogen.

X-ray diffraction data were collected using synchrotron radiation on the SER-CAT beamline of the Advanced Photon Source (APS), Argonne National Laboratory (ANL), Argonne, Illinois, USA at 100 K using MAR CCD detectors. Data frames were indexed and diffraction spots were integrated and scaled using the *HKL*-2000 program package (Otwinowski & Minor, 1997). Structure solutions were obtained using the *CCP*4 program package (Winn *et al.*, 2011).

3. Results and discussion

3.1. Crystallization of Fab and diffraction study of Fab crystals

Crystals of the Fab fragment were grown in conditions consisting of 10%(*v*/*v*) 2-propanol, 100 m*M* sodium citrate pH 5.0, 26%(*v*/*v*) polyethylene glycol 400 (PEG 400). Because of the presence of a high concentration of PEG 400, the crystals could readily be cooled in liquid nitrogen without additional cryoprotectant for X-ray diffraction data collection. Fab crystals typically appeared 3 d after crystallization setup and grew to their maximal size within two weeks (Fig. 1*a*). The best crystal diffracted X-rays to 1.75 Å resolution using synchrotron X-ray radiation (Fig. 1*b*, Table 1). The crystals of the Fab from MORAb-009 belonged to the tetragonal crystal system, with unit-cell parameters $a = b = 140.6$, $c = 282.0$ Å and with a possible space-group symmetry of either $P4_32_12$ or $P4_12_12$. Matthews coefficient analysis (Matthews, 1968) suggested four Fab molecules per crystallographic asymmetric unit ($V_{\rm M} = 3.7$ Å^3 Da^{-1}, 66.7% solvent content). The structure was solved by the molecular-replacement method using the *BALBES* program (Long *et al.*, 2008) in the *CCP*4 program suite (Winn *et al.*, 2011). The coordinates of the Fab fragment derived from Mab-IA (PDB entry 1a6t; Che *et al.*, 1998), a monoclonal antibody that neutralizes human rhinovirus 14, were used as a phasing template, which gave rise to a solution with four Fab molecules in the asymmetric unit in space group $P4_12_12$. The solution has a Q factor of 0.802 and a 'probability to be a solution' of 99%.

3.2. Crystallization of Fab–Msln7-64 complex

It has been shown that the N-terminal 64-residue fragment of mesothelin is responsible for CA-125 recognition (Kaneko *et al.*, 2009) and that this interaction can be interrupted by MORab-009 (Hassan *et al.*, 2010). From these experiments, it was inferred that the

64-residue fragment adopts a fixed conformation. We were able to narrow down the residue range of the minimal fragment capable of reacting with the antibody to residues 7–60. Crystals of the Fab–Msln7-64 complex were grown in simple conditions consisting of 100 m*M* trisodium citrate pH 5.6, 17%(*v*/*v*) PEG 3350. Crystals appeared 2 d after setup and grew to their mature size in about 10 d (Fig. 2*a*). To confirm the molecular composition of these crystals, a large single crystal was selected, washed thoroughly in the well solution and subjected to SDS–PAGE analysis under nonreducing conditions. The PAGE gel was silver stained and showed the presence of both Fab (50 kDa) and Msln7-64 (7 kDa) fragments, thus establishing the molecular identity of these crystals (Fig. 2*b*). There were minor bands on the gel stemming from impurities that were mostly introduced by the Msln7-64 sample. However, these minor bands were significantly reduced compared with the purified sample, suggesting that the crystallization process can serve as a purification step. The higher molecular-weight band that was present in the crystal sample was not present in the purified complex.

To collect diffraction data under cooled conditions, Fab–Msln7-64 complex crystals were soaked for a short period of time in a cryoprotectant solution consisting of 100 m*M* trisodium citrate pH 5.6, 17%(*v*/*v*) PEG 3350 supplemented with 20% ethylene glycol and cooled in liquid nitrogen.

3.3. X-ray diffraction analysis of Fab–Msln7-64 complex crystals

Cooled Fab–Msln7-64 crystals diffracted X-rays to 2.6 Å resolution at a synchrotron-radiation source (Fig. 2*c*, Table 1). These crystals belonged to the hexagonal crystal system, with unit-cell parameters $a = b = 146.2$, $c = 80.9$ Å, $\gamma = 120^\circ$. The Matthews coefficient (V_M) for one complex molecule per crystallographic asymmetric unit was 4.7 Å^3 Da^{-1}, with a solvent content of 74.0%. Analysis of systematic absences of reflections suggested that these complex crystals possessed the symmetry of space group $P6_2$ or $P6_4$. The crystal structure was solved in space group $P6_4$ by the molecular-replacement method using the atomic coordinates of the MORAb-009 Fab fragment as a search model using the program *MOLREP* (Vagin & Teplyakov, 2010) in the *CCP*4 suite, which produced an initial *R* factor of 0.456 using reflections in the resolution range 50–2.9 Å. Since the N-terminal fragment of mesothelin is only 7 kDa, which is approximately 12% of the unit-cell content, electron densities that were not part of the Fab structure were clearly visible and were assigned to the mesothelin molecule. Model building and refinement is currently under way.

The authors wish to thank the staff of the SER-CAT beamline at APS, ANL for their assistance in data collection. This research was supported by the Intramural Research Program of the NIH, National Cancer Institute, Center for Cancer Research and by a CRADA with Morphotek Inc. We also thank George Leiman for his editorial assistance during the preparation of this manuscript.

References

Bast, R. C., Xu, F. J., Yu, Y. H., Barnhill, S., Zhang, Z. & Mills, G. B. (1998). *Int. J. Biol. Markers*, **13**, 179–187.
Bateman, A. C., al-Talib, R. K., Newman, T., Williams, J. H. & Herbert, A. (1997). *Histopathology*, **30**, 49–56.
Chang, K. & Pastan, I. (1996). *Proc. Natl Acad. Sci. USA*, **93**, 136–140.
Che, Z., Olson, N. H., Leippe, D., Lee, W., Mosser, A. G., Rueckert, R. R., Baker, T. S. & Smith, T. J. (1998). *J. Virol.* **72**, 4610–4622.
Chowdhury, P. S. & Pastan, I. (1999). *Nature Biotechnol.* **17**, 568–572.
Hassan, R., Bera, T. & Pastan, I. (2004). *Clin. Cancer Res.* **10**, 3937–3942.
Hassan, R. *et al.* (2007). *Cancer Immun.* **7**, 20.
Hassan, R., Schweizer, C., Lu, K. F., Schuler, B., Remaley, A. T., Weil, S. C. & Pastan, I. (2010). *Lung Cancer*, **68**, 455–459.
Ho, M., Bera, T. K., Willingham, M. C., Onda, M., Hassan, R., FitzGerald, D. & Pastan, I. (2007). *Clin. Cancer Res.* **13**, 1571–1575.
Ho, M., Hassan, R., Zhang, J., Wang, Q., Onda, M., Bera, T. & Pastan, I. (2005). *Clin. Cancer Res.* **11**, 3814–3820.
Kaneko, O., Gong, L., Zhang, J., Hansen, J. K., Hassan, R., Lee, B. & Ho, M. (2009). *J. Biol. Chem.* **284**, 3739–3749.
Kojima, T., Oh-eda, M., Hattori, K., Taniguchi, Y., Tamura, M., Ochi, N. & Yamaguchi, N. (1995). *J. Biol. Chem.* **270**, 21984–21990.
Long, F., Vagin, A. A., Young, P. & Murshudov, G. N. (2008). *Acta Cryst.* D**64**, 125–132.
Matthews, B. W. (1968). *J. Mol. Biol.* **33**, 491–497.
Otwinowski, Z. & Minor, W. (1997). *Methods Enzymol.* **276**, 307–326.
Pastan, I., Hassan, R., FitzGerald, D. J. & Kreitman, R. J. (2006). *Nature Rev. Cancer*, **6**, 559–565.
Rump, A., Morikawa, Y., Tanaka, M., Minami, S., Umesaki, N., Takeuchi, M. & Miyajima, A. (2004). *J. Biol. Chem.* **279**, 9190–9198.
Sathyanarayana, B. K., Hahn, Y., Patankar, M. S., Pastan, I. & Lee, B. (2009). *BMC Struct. Biol.* **9**, 1.
Vagin, A. & Teplyakov, A. (2010). *Acta Cryst.* D**66**, 22–25.
Winn, M. D. *et al.* (2011). *Acta Cryst.* D**67**, 235–242.
Yen, M. J., Hsu, C.-Y., Mao, T.-L., Wu, T.-C., Roden, R., Wang, T.-L. & Shih, I.-M. (2006). *Clin. Cancer Res.* **12**, 827–831.